



Cite this: *J. Anal. At. Spectrom.*, 2023, **38**, 97

Development of a single method for direct measurement of multiple radionuclides using ICP-MS/MS

B. C. Russell,^a P. E. Warwick,^{b,c} H. Mohamud,^a O. Pearson,^a Y. Yu,^d H. Thompkins,^a S. L. Goddard,^e I. W. Croudace^c and Z. Zacharauskas^{ac}

Tandem inductively coupled plasma mass spectrometry (ICP-MS/MS) has demonstrated effective online removal of interferences for a number of medium and long-lived radionuclides including ^{90}Sr , ^{129}I , ^{137}Cs and ^{237}Np . This reduces or removes the dependence on relatively time consuming offline chemical separation, improving sample throughput and offering economic benefits for end users through reduced procedural time, analyst time, secondary waste arisings and quantity of resins and reagents required. This work demonstrates the development and application of a method for measuring multiple radionuclides (including ^{63}Ni , ^{90}Sr , ^{93}Zr , ^{99}Tc , ^{129}I , ^{237}Np , ^{239}Pu) and stable elements in various sample matrices in a single measurement. Separate instrument modes customised for individual radionuclides were combined into a single run, each using a different instrument setup depending on the extent of interference removal required. The measurement time was approximately seven minutes and consumed 3.5 mL for each sample. Instrument conditions were optimised for each radionuclide using stable and radioactive standards, and then validated using samples including aqueous wastes from a nuclear site, air filters following microwave dissolution, groundwater, and soil, sediment and concrete samples following borate fusion dissolution. Matrix-matched calibration standards were prepared, and a multi-element standard solution was used as an internal standard. The limits of detection were compared to regulatory limits, which showed that longer-lived radionuclides such as ^{93}Zr , ^{99}Tc , ^{129}I and ^{237}Np can be directly measured, whilst shorter-lived radionuclides such as ^{90}Sr and ^{63}Ni require separation and pre-concentration prior to sample introduction. The method provides a significant amount of information on stable and radioactive composition in a single measurement, with the potential to further expand the number of radionuclides measurable as part of this single procedure.

Received 20th May 2022
Accepted 21st September 2022

DOI: 10.1039/d2ja00174h

rsc.li/jaas

1. Introduction

Inductively coupled plasma mass spectrometry (ICP-MS) has been proven to offer a rapid alternative to traditional alpha and beta decay counting techniques for medium and long-lived radionuclides for a number of applications. Several reviews have been published on the role of ICP-MS for radionuclide measurement.^{1–3} ICP-MS is increasingly recognised as the preferred method for medium and long-lived radionuclide measurement due to favourable sensitivity, speed and sample preparation compared to alpha and beta counting techniques. Accurate measurement of radionuclides requires the removal of

multiple interferences, specifically; isobaric interferences produced by stable or radioactive isotopes at the similar mass to the analyte of interest *e.g.* ^{129}Xe on ^{129}I ; polyatomic interferences formed by reactions of ions with other species in the ICP-MS, producing ions (such as hydrides, oxides and argides) with a similar mass to the analyte that cannot be distinguished by the instrument *e.g.* $^{97}\text{Mo}^{16}\text{O}_2$ on ^{129}I ; peak tailing interferences from a stable or radioactive isotope at a similar mass to the analyte with a significantly higher concentration, which can then overlap onto the analyte signal. If the tailing isotope is from the same element as the analyte, these cannot be separated by chemical means *e.g.* ^{127}I on ^{129}I .

Of the available instrumentation, tandem ICP-MS/MS has demonstrated an improvement in instrument-based interference removal, reducing the reliance on time-consuming offline chemical separation. ICP-MS/MS consists of two quadrupole mass filters, separated by a collision-reaction cell. The use of a collision or reaction gas can selectively remove polyatomic and isobaric interferences, respectively, whilst operating with two quadrupole mass filters means the peak tailing removal

^aNuclear Metrology, National Physical Laboratory, Hampton Road, Teddington, TW11 0LW, UK. E-mail: ben.russell@npl.co.uk

^bGAU Radioanalytical, UK

^cUniversity of Southampton, NOCS, Southampton, SO14 3ZH, UK

^dRoyal Holloway University of London, Egham Hill, Egham, TW20 0EX, UK

^eAir Quality and Aerosol Metrology, National Physical Laboratory, Hampton Road, Teddington, TW11 0LW, UK



capability is greater than that of single quadrupole instruments, with values on the order of $<10^{-10}$ achievable. Additionally, positioning a quadrupole before the entrance to the cell enables the sample to be mass filtered prior to entering the cell, simplifying the cell chemistry. This technique has been applied to the measurement of multiple radionuclides including ^{90}Sr , ^{129}I , $^{135}\text{Cs}/^{137}\text{Cs}$, ^{226}Ra and $^{236}\text{U}/^{238}\text{U}^{4-11}$ and its capabilities for nuclear waste characterisation has been recently reviewed.¹² The combination of MS/MS mode with a collision-reaction cell increases user confidence in the direct measurement of samples without relying on offline separation prior to measurement.

Whilst difficult-to-measure radionuclides have been effectively measured using ICP-MS/MS, the combination of multiple instrument modes into a single procedure has not been utilised. Using the instrument software, it is possible to combine different modes to enable the measurement of multiple radionuclides in a single run. For example, measurement of a radionuclide that benefits from the use of O_2 as a reaction gas (such as ^{90}Sr)¹³ can be followed by measurement of a radionuclide that benefits from NH_3 (such as ^{93}Zr),^{14,15} and then no gas (e.g. ^{237}Np)¹² and so on as part of a single run. This approach provides more information from a single measurement.

This study shows the development of optimised methods for multiple radionuclides, initially using single radionuclide standards and then spiking with increasing concentrations of interferences. These individual methods are then combined into a single procedure along with the stable element composition and tested for direct measurement of various samples. The limit of detection achieved is compared to regulatory limits to assess which radionuclides can be directly measured, and which require further sample preparation steps. Consideration is also given for additional radionuclides that can be measured as part of this single procedure.

2. Methodology

2.1. Reagents

Nitric acid (Fisher Scientific, Trace Analysis Grade) was diluted to 0.2 M in deionised water (ELGA, Veolia Water, Marlow, UK, 18 M Ω cm/5 ppb Total Organic Carbon). Stable single element standards (Sigma Aldrich and Romil, 100–10 000 $\mu\text{g g}^{-1}$) and NPL radionuclide standards were used for custom tuning of the ICP-MS/MS. Borate fusion dissolution of solid materials used pre-mixed lithium borate (49.75% lithium tetraborate–49.75% lithium metaborate–0.5% lithium bromide (Spex)).

2.2. Instrumentation

An Agilent 8800 ICP-MS/MS was used for this work. The instrument was fitted with a quartz double-pass spray chamber, Micromist nebuliser and nickel sample and skimmer cones. The instrument can be operated in Single Quad (SQ) mode (with only the second mass filter (Q2) operating) or MS/MS mode (both Q1 and Q2 mass filters operating). The collision/reaction cell can be operated in either Single Quad or MS/MS mode. The dual mode SEM detector has a range of nine orders of

Table 1 Cell gas properties for the Agilent 8800

Cell gas line	Cell gas	Flow rate (mL min ⁻¹)
Hydrogen	H_2	0.5–10
Helium	He	0.5–12
Cell line 3	Corrosive gas ^a e.g. NH_3 , CH_3F	0.5–10
Cell line 4	Non-corrosive gas e.g. O_2 , N_2O , NO_2	0.05–1.0

^a When operating the corrosive gas line, the He line automatically runs at a flow rate of 1 mL min⁻¹ to protect the collision/reaction cell

magnitude and can be used for isotopic ratio measurements, although this isn't the focus of this study.

The Agilent 8800 has 4 cell gas lines (Table 1). In this study, NH_3 was introduced *via* the corrosive gas line, and O_2 *via* the non-corrosive gas line. To prevent NH_3 from damaging the collision/reaction cell, the gas mixture is 10% NH_3 in 90% He. Additionally, the He gas line automatically runs at a flow rate of 1 mL min⁻¹ when the corrosive gas line is operating to protect the cell. Helium, O_2 and NH_3 gases were provided by BOC, and hydrogen was provided from a generator (Linde NM Plus), all with a purity of N 6.0 (99.9999%).

The instrument was tuned daily in all modes using a mixed 1 ng g⁻¹ standard solution. The sensitivity across the mass range was assessed at ^9Be , ^{89}Y and ^{205}Tl , with the oxide and doubly charged ratio assessed by $^{140}\text{Ce}^{16}\text{O}/^{140}\text{Ce}$ and $^{140}\text{Ce}^{2+}/^{140}\text{Ce}^+$ ratios, respectively. The quality control of the instrument was performed by generating a tune report each time the instrument was run, and the results logged in a control chart to ensure the sensitivity and uncertainty thresholds were reached, and that oxide and doubly charged ion formation was <2%. The peak axes at $m/z = 9$, 89 and 205 were also assessed to ensure the peak was within 0.1 atomic mass unit e.g. 8.9–9.1 for $m/z = 9$.

For radionuclide-specific measurement, the instrument was custom tuned by manually adjusting instrument parameters, focusing on the properties of the collision/reaction cell to find the best balance between sensitivity and interference removal. Firstly, the cell gas flow rate for the one or more gases used for each radionuclide; the octopole bias voltage, which impacts the acceleration and kinetic energy of ions in the cell; and the energy discrimination voltage, which provides an energy barrier at the exit of the cell for filtering out interferences whilst retaining analyte ions. When using NH_3 , a range of cell product ions can be formed (NH^+ , NH_2^+ etc.). This was initially assessed by performing a product ion scan using single element standards. Q1 is set to a single m/z value (e.g. 63 for Ni), and Q2 then measures all m/z values up to 260, with each peak representing a cell product that can then be investigated further. For samples with an unknown composition, a precursor ion scan can also be applied where Q2 is set to a single m/z value and the Q1 mass range is scanned to determine if interfering elements are present in the sample.

A Spex Katanax K2 Prime was used for borate fusion dissolution of soil, sediment and concrete samples. An Anton Paar Multiwave 3000 microwave oven was used for dissolution of filter samples.



Table 2 Properties of radionuclides measured in this study

Radionuclide	Half life (a)	Production route	Principal decay mode	Mass equivalent to an activity of 1 Bq (pg)	Decay counting measurement technique
⁶³ Ni	98.7(24)	Activation	β	0.5	Liquid scintillation counting (LSC)
⁹⁰ Sr	28.8(7)	Fission	β	0.2	LSC
⁹³ Zr	$1.61(6) \times 10^6$	Fission and activation	β	1.1×10^4	LSC
⁹⁹ Tc	$2.1(11) \times 10^5$	Fission	β	1.6×10^3	LSC
¹²⁹ I	$16.1(7) \times 10^6$	Fission	β	1.6×10^5	LSC
²³⁷ Np	$2.1(7) \times 10^6$	Neutron capture	α	3.8×10^4	Alpha spectrometry
²³⁹ Pu	$24.1(11) \times 10^3$	Neutron capture	α	4.4×10^2	Alpha spectrometry

Table 3 Summary of interferences affecting ICP-MS measurement of radionuclides of interest

Radionuclide	Isobar (% abundance)	Major polyatomics	Tailing (% abundance)
⁶³ Ni	⁶³ Cu (69.15)	⁶² Ni ¹ H, ⁴⁹ Ti ¹⁴ N, ⁴⁷ Ti ¹⁶ O, ³¹ P ³² O, ³⁵ Cl ²⁸ Si, ²⁷ Al ³⁶ Ar, ²⁵ Mg ³⁸ Ar, ²³ Na ⁴⁰ Ar	⁶² Ni (3.63) ⁶⁴ Zn (48.27)
⁹⁰ Sr	⁹⁰ Zr (51.45)	⁸⁹ Y ¹ H, ⁷⁴ Ge ¹⁶ O, ⁵⁹ Ni ¹⁶ O ₂ , ⁵⁰ Ti ⁴⁰ Ar, ⁵⁰ V ⁴⁰ Ar, ⁵⁴ Fe ³⁶ Ar	⁸⁸ Sr (82.58)
⁹³ Zr	⁹³ Nb (100)	⁹² Zr ¹ H, ⁷⁷ Se ¹⁶ O, ⁶¹ Ni ¹⁶ O ₂ , ⁵³ Cr ⁴⁰ Ar	⁹² Zr (17.15)
⁹⁹ Tc	⁹⁹ Ru (12.76)	⁹⁸ Mo ¹ H, ⁸³ Kr ¹⁶ O, ⁶⁴ Zn ³⁵ Cl, ⁵⁹ Co ⁴⁰ Ar, ⁵¹ V ¹⁶ O ₃	⁹⁸ Mo (24.19) ¹⁰⁰ Mo (9.67) ¹⁰⁰ Ru (12.60)
¹²⁹ I	¹²⁹ Xe (26.40)	¹²⁷ IH ₂ , ⁹⁷ MoO ₂ , ¹¹³ Cd ¹⁶ O, ¹¹⁵ In ¹⁴ N, ⁸⁹ Y ⁴⁰ Ar	¹²⁷ I (100)
²³⁷ Np	—	²⁰⁵ Tl ¹⁶ O ₂ , ¹⁹⁷ Au ⁴⁰ Ar	²³⁸ U (99.27)
²³⁹ Pu	—	²³⁸ U ¹ H	²³⁸ U (99.27)

2.3. Experimental

2.3.1. Radionuclides of interest. Radionuclides were selected based on (1) their importance with regards to accurate detection for waste characterisation, decommissioning and/or environmental monitoring and (2) suffering from significant interferences that could benefit from the ICP-MS/MS setup. There are multiple fission and/or activation products (Table 2) covering a range of masses, half-lives, and interferences (Table 3), and therefore will give a good overview of ICP-MS/MS capabilities for radionuclide measurement. Methods developed for additional radionuclides are discussed in Section 3.1.3. It should be noted that there are a range of potential polyatomic interferences for all radionuclides. Major ones have been noted in Table 3, but the composition of the starting sample should be assessed for each sample type to determine the interferences present.

2.3.2. Measurement of standards. Where possible, sensitivity was initially assessed using stable element standards. For radionuclide measurements, samples were prepared from NPL standards using a dedicated source preparation facility. A stock solution was prepared, and calibration standards were prepared by gravimetric dilution of the stock solution using 0.2 M HNO₃. The volatile nature of iodine means it must be introduced in alkali media, in this study 0.001 M NaOH was used.

For each radionuclide, the instrument was run in different modes to determine the impact on sensitivity and interference removal capability. This was initially assessed using interference-free solutions, followed by spiking with various concentrations of known interferences. Each collision and reaction gas was tested, along with the difference between

Single Quad and MS/MS mode. For higher matrix samples, the instrument can be operated with argon gas aerosol dilution (termed High Matrix Introduction or HMI) throughout, which allows tolerance of high matrix samples (up to 2.5% total dissolved solids) and is a faster alternative to offline dilution.

2.3.3. Development of a combined procedure. Once the instrument setup had been optimised for individual radionuclides, each mode was combined into a single procedure that would enable determination of multiple radionuclides in a single measurement. Up to eight modes can be used in a single measurement, which in this study consisted of seven radionuclides and the stable element composition. The stable composition mode operates in MS/MS mode with He collision gas at a flow rate of 4 mL min⁻¹ and can therefore also be used to measure radionuclides that do not suffer from significant interferences (see Section 3.1.3). Depending on the radionuclides of interest to the sample matrix being tested, the modes used can be varied.

2.3.4. Testing of combined procedure. The combined procedure was tested using various samples, with the aim of determining the difference between the instrument limit of detection (LOD) for radionuclide standards using an instrument blank (the solution the radionuclide standard was prepared in), and the method LOD for real samples using a sample blank. In both cases, the LOD is calculated as the equivalent concentration of three times the standard deviation of the blank. The results would show which radionuclides could potentially be measured directly at suitably low activities without sample preparation, and which radionuclides require chemical separation prior to sample introduction. Results are expressed throughout for both mass and activity.



Aqueous waste samples were provided from a UK nuclear site. Some contained radionuclides of interest for this study, others were spiked with radionuclide standards of interest over a range of activity concentrations. These were measured without prior sample preparation. Twelve groundwater samples from sites around the UK were received from the British Geological Survey, and after filtering were also tested by taking a 1 mL aliquot and diluting to 10 mL in 0.2 M HNO₃.

Air filter samples were provided by the NPL Air Quality and Aerosol Metrology Group, who are responsible for operating the UK Metals Monitoring Network on behalf of the Environment Agency and the UK governmental Department for Environment, Food and Rural Affairs (Defra). The Network consists of monitoring sites all around the UK that sample airborne particulate matter with an aerodynamic diameter less than 10 µm (PM10) onto cellulose ester filters. The sampled filters from the monitoring sites were prepared for analysis by microwave digestion. The filters were digested in a mixture of hydrogen peroxide and nitric acid. After digestion, the solutions were diluted to a total volume of 50 mL in deionised water, then analysed by ICP-MS for a suite of twelve metals to be reported for the Network analysis.¹⁶ In this study, four of these samples originally prepared for Network analysis were measured to assess the potential of the combined procedure for measurement of radionuclides on air filter samples.

Several solid samples (soil, sediment, concrete) were measured following lithium borate fusion, a dissolution technique first used in the radioanalytical field by Croudace *et al.* (1998).¹⁷ The method is described in detail elsewhere.¹⁸ Briefly, a 1 g sample was added to a crucible (95% Pt/5% Au) along with 1 g of 49.75/49.75/0.5 lithium metaborate/lithium tetraborate/lithium bromide, which was mixed manually. Each sample was loaded onto an automated fusion furnace (Spex Katanax K2 Prime) for dissolution. The fused samples were automatically dispensed by the instrument into PTFE beakers containing 50 mL 4 M HNO₃ with a PTFE magnetic stirrer to aid dissolution of the flux. The total time to prepare and digest a batch of five samples was approximately 40 minutes. A 1 mL aliquot of the dissolved flux was diluted to 50 mL with 0.2 M HNO₃ and measured without further treatment.

3. Results and discussion

More detailed information is given on instrument optimisation for ⁶³Ni and ⁹⁹Tc, where there has been limited application of ICP-MS/MS. The optimal instrument setup for all radionuclides was determined in the same way and are summarised in Section 3.1.3 for those that have been published elsewhere.

3.1. Measurement of standards

3.1.1. Nickel-63. Nickel-63 is measurable by LSC following chemical separation, achieved by dimethylglyoxime (DMG) precipitation, anion exchange and/or extraction chromatography.^{19–24} Whilst not being a focus of this study, there is additional interest in measurement of longer lived ⁵⁹Ni (half life 76 (5) × 10³ a), which has the potential to be a powerful forensic

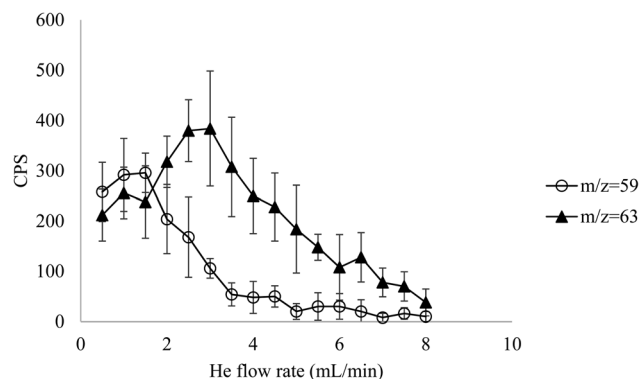


Fig. 1 Background at $m/z = 63$ and $m/z = 59$ with increasing He flow rate to determine isobaric and polyatomic background interferences.

tool through measurement of ⁵⁹Ni/⁶³Ni isotopic ratios. Whilst theoretically measurable, ⁵⁹Ni suffers from significant tailing (⁵⁸Ni), polyatomic (⁵⁸Ni¹H) and isobaric (⁵⁹Co) interferences and there is no known ICP-MS procedure for measuring this radionuclide.

Measurement of both stable and radioactive Ni isotopes by ICP-MS/MS has been demonstrated elsewhere, using a combination of NH₃ and H₂ to achieve separation from isobaric ⁶³Cu through selective formation of Ni(NH₃)₃.²⁵ In the case of ⁶³Ni, operating in MS/MS mode improves tailing removal from ⁶²Ni, although the low isotopic abundance (3.6%) means this is unlikely to be an issue. The main advantage of operating in MS/MS mode is filtering the ion beam to $m/z = 63$ prior to using NH₃ cell gas, simplifying the cell chemistry where a number of potential products can be formed.

The relatively short half life of ⁶³Ni with regards to ICP-MS measurement (1 Bq g⁻¹ is equivalent to 0.5 pg g⁻¹) means operating in MS/MS mode and using cell gas must be more carefully considered for its impact on sensitivity compared to longer-lived radionuclides.

When He cell gas was introduced, the background at $m/z = 63$ increased up to a flow rate of 3 mL min⁻¹, followed by a decrease at higher gas flow rates (Fig. 1). The increase is likely a result of collisional focusing, which is evidence of an isobaric interference, in this case ⁶³Cu. The background at $m/z = 59$ was also measured because of interest in potential ⁵⁹Ni measurement. The background increased slightly from 0.5–1.5 mL min⁻¹ before decreasing at higher gas flow rates. This slight increase is associated with stable ⁵⁹Co, which overlaps with ⁵⁹Ni, however, the decrease in signal at higher He flow rates is indicative of a polyatomic interference (most likely ⁵⁸Ni¹H) that is not affected by collisional focusing.

Oxygen cell gas was investigated, however, a limited amount of NiO was formed (maximum 6% compared to the CPS measured for Ni on-mass), increasing to 12% when the energy discrimination and octopole bias were custom tuned. By comparison, 0.5% of the total Cu signal was measured as CuO under the same conditions, suggesting a decontamination factor of 10 was achievable. Using NH₃ cell gas alone, a Ni/Cu formation rate of 35 (calculated as the CPS for stable



Table 4 Impact of $\text{NH}_3 + \text{H}_2$ on Ni and Cu sensitivity (CPS for a 1 ng g^{-1} solution) compared to NH_3 only (all other instrument parameters unchanged)

NH_3 (mL min^{-1})	H_2 (mL min^{-1})	$\text{Ni}(\text{NH}_3)_3$ (CPS)	$\text{Cu}(\text{NH}_3)_3$ (CPS)
2.0	0	3900	70
	0.5	6500	110
	1.0	6800	130
	1.5	7200	140
	2.0	7100	125
	2.5	7100	120
	3.0	6600	130

$^{58}\text{Ni}(\text{NH}_3)_3/^{63}\text{Cu}(\text{NH}_3)_3$, with isotopic abundance scaled to 100% for each element) was achieved at a flow rate of 3 mL min^{-1} , further improved by decreasing the energy discrimination from a starting value of -7 V to -13 V . The starting octopole bias value of -4.5 V was determined to be optimal.

Compared to NH_3 alone, the addition of H_2 gas increased $\text{Ni}(\text{NH}_3)_3$ formation up to a flow rate of 1.5 mL min^{-1} . There was also an increase in $\text{Cu}(\text{NH}_3)_3$ formation (Table 4) but the Ni/Cu separation factor remained constant. The Ni/Cu separation factor was improved to 100 at 1 mL min^{-1} NH_3 and 3 mL min^{-1} H_2 , with a sensitivity of 6100 CPS for a 1 ng g^{-1} ($2.1 \times 10^3 \text{ Bq g}^{-1}$) Ni solution. At 1 mL min^{-1} NH_3 only, the Ni/Cu separation factor was 90–95, but the Ni sensitivity was significantly lower (15 CPS). Under optimised conditions (Fig. 2), the ^{63}Ni detection limit was calculated as 0.52 Bq g^{-1} (0.25 pg g^{-1}), with the background at $m/z = 63 < 10 \text{ CPS}$, compared to 500 CPS in no-gas mode.

3.1.2. Technetium-99. Technetium-99 has been effectively measured using LSC^{26,27} and increasingly by ICP-MS.^{28–30} In both cases, measurement is preceded by chemical separation, with effective techniques including co-precipitation,^{31,32} solvent extraction,^{31,33} anion exchange³⁴ and extraction chromatography using TEVA resin^{35–37} and more recently TK201 resin.³⁸ Both ^{97}Tc and ^{98}Tc are suitable long-lived tracers, with ^{97}Tc favoured because of the possibility of $^{98}\text{Tc}^1\text{H}$ polyatomic formation overlapping at $m/z = 99$. Unfortunately, this is not commercially available, and to date, chemical yield has been calculated through measurement of short-lived isotopes *e.g.* ^{95}Tc or $^{99\text{m}}\text{Tc}$ using gamma spectrometry, or stable Re.

Whilst ICP-MS/MS has been applied to ^{99}Tc ,³⁹ this was following chemical separation, and the possibility of cell-based

interference removal has not been investigated. Operating in MS/MS mode could improve tailing removal from ^{98}Mo , whilst the use of cell gases may be used to remove isobaric ^{99}Ru and polyatomic $^{98}\text{Mo}^1\text{H}$. The instrument blank at $m/z = 99$ was 0–5 CPS in 0.2 M HNO_3 solutions. Operating in MS/MS mode with no cell gas reduced the sensitivity by 50% compared to Single Quad mode (245 000 and 450 000 CPS for 1 Bq g^{-1} ($1.6 \times 10^3 \text{ pg g}^{-1}$), respectively). However, the peak tailing removal was improved, with MS/MS mode able to tolerate up to $1 \mu\text{g g}^{-1}$ ^{98}Mo before the signal increased at $m/z = 99$. The use of He as a collision gas was very effective at reducing the signal from polyatomic $^{98}\text{Mo}^1\text{H}$, with the signal from a $10 \mu\text{g g}^{-1}$ Mo solution reducing from 2200 CPS at 0.5 mL min^{-1} to $<5 \text{ CPS}$ at 8 mL min^{-1} . However, the use of collision gas did not offer separation from isobaric ^{99}Ru and was not considered further.

A product ion scan using NH_3 (3 mL min^{-1}) showed the majority of Tc remained on mass (90%). Whilst multiple cell products were formed, in all cases the sensitivity was low, with a maximum of 2.4% of the total counts for a mass shift of 34 ($\text{Tc}(\text{NH}_3)_2$). The majority of Mo and Ru also remained on mass under the same conditions (85% and 80%, respectively). The shift from $m/z = 99$ to 185 ($\text{TcH}(\text{NH}_3)_5^+$) was the most promising for Ru/Mo separation. Custom tuning of the cell parameters improved Tc sensitivity to $3 \times 10^3 \text{ CPS}$, whilst the signal from 10 ng g^{-1} Ru was reduced by an order of magnitude from $5 \times 10^2 \text{ CPS}$ to $3.6 \times 10^1 \text{ CPS}$. However, accompanied with this was the increase of the Mo signal by an order of magnitude, from $2.4 \times 10^1 \text{ CPS}$ to $1.2 \times 10^2 \text{ CPS}$. This mode offers the optimal Ru decontamination, however, the Tc sensitivity remained low and contamination from Mo remained.

In O_2 mode, Tc remained predominantly on-mass over an O_2 flow rate of $0.1\text{--}0.7 \text{ mL min}^{-1}$, with collisional focusing improving sensitivity by 65% from 0.10 mL min^{-1} up to 0.35 mL min^{-1} O_2 before decreasing at higher flow rates. The shift from Tc to TcO ranged from 1% to 15% of the total Tc signal, peaking at 0.45 mL min^{-1} O_2 . The TcO_2 shift also ranged from 1% to 15%, with an optimal O_2 flow rate of 0.45 mL min^{-1} . Additionally, the background at $m/z = 131$ (TcO_2) was 0 CPS. A mixture of 10 ng g^{-1} Ru and $1 \mu\text{g g}^{-1}$ Mo was run in the optimised modes for measurement of ^{99}Tc , $^{99}\text{Tc}^{16}\text{O}$ and $^{99}\text{Tc}^{16}\text{O}_2$ to determine the decontamination achievable. When measuring Tc as $^{99}\text{Tc}^{16}\text{O}_2$, the ^{99}Ru and $^{98}\text{Mo}^1\text{H}$ interferences were effectively suppressed compared to other modes. There was limited

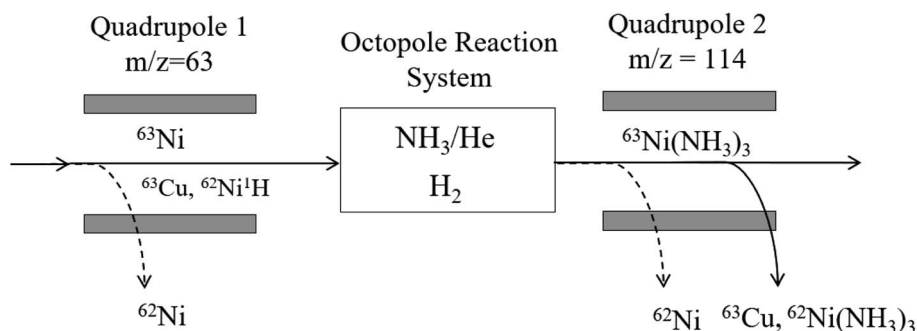


Fig. 2 Instrument layout for measurement of ^{63}Ni .



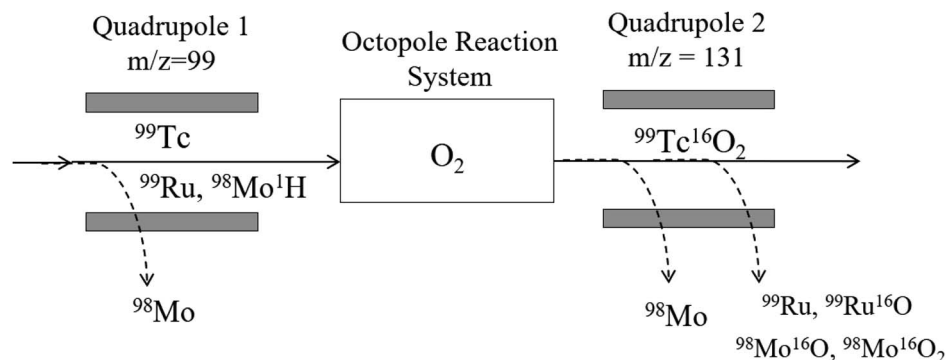


Fig. 3 Instrument layout for measurement of ^{99}Tc .

formation of $^{99}\text{Ru}^{16}\text{O}_2$, whilst $^{98}\text{Mo}^{16}\text{O}_2$ readily formed $^{98}\text{Mo}^{16}\text{O}_2$, but limited $^{98}\text{Mo}^{16}\text{O}_2^{16}\text{O}$. Measurement of ^{99}Tc as $^{99}\text{Tc}^{16}\text{O}_2$ therefore effectively changed an interfering polyatomic into another, non-interfering polyatomic in the case of $^{98}\text{Mo}^{16}\text{O}_2$. Generally, custom tuning of the instrument was effective at suppressing $^{98}\text{Mo}^{16}\text{O}_2$, but behaviour of Ru and Tc was similar. The Tc sensitivity was improved from 2.5×10^4 CPS per Bq g^{-1} to 3.8×10^4 CPS per Bq g^{-1} when optimised, however, the background contribution from Ru increased by a factor of 5, to approximately 500 CPS at a concentration of 10 ng g^{-1} . It was therefore decided that the best compromise between sensitivity and interference removal was to use the 'standard' O_2 auto-tune settings. A summary of the performance of different cell gases is shown in Table 5. In the optimised setup (Fig. 3), the instrument LOD for ^{99}Tc was 0.3 mBq g^{-1} , equivalent to 0.5 pg g^{-1} .

3.1.3. Other radionuclides. Methods have been developed for several other radionuclides that are relevant to this study, which are published in detail elsewhere. Strontium-90 has been increasingly measured by ICP-MS over the past 20 years, with the main advantage being a shorter measurement time compared to LSC.^{40–43} ICP-MS/MS has been proven to offer improved interference removal compared to alternative instrument designs.^{4,5,13,44} The additional mass filter improved tailing removal of ^{88}Sr , and the majority of studies favour the use of O_2 to remove isobaric ^{90}Zr through the formation of $^{90}\text{Zr}^{16}\text{O}$, whilst ^{90}Sr remains on mass. The formation of in-cell oxide interferences (e.g. $^{74}\text{Ge}^{16}\text{O}$ and $^{58}\text{Ni}^{16}\text{O}_2$) is limited by setting Q1 to $m/z = 90$. ICP-MS/MS has been applied to ^{90}Sr measurement in samples including soils contaminated by the Fukushima accident⁴⁴ and urine,⁵ with measurement generally preceded by multi-stage chemical separation.

ICP-MS/MS has been demonstrated as a viable method for measurement of ^{93}Zr .^{14,15} A combination of NH_3 and H_2 gases was shown to offer the most efficient separation from stable isobaric ^{93}Nb and radioactive ^{93}Mo , through the selective formation of $^{93}\text{Zr}(\text{NH}_3)_6$, measured at $m/z = 195$. After demonstrating this using stable and radioactive standard solutions,¹⁴ the method was modified for dissolved steel and aqueous waste samples,¹⁵ with detection limits of $1.1\text{--}8.3 \text{ pg g}^{-1}$ ($0.1\text{--}0.8 \text{ mBq g}^{-1}$).

Iodine-129 has been measured by ICP-MS/MS in samples contaminated by the Fukushima Nuclear Power Plant

accident.^{45,46} In all cases, O_2 gas was used to minimise the interference from isobaric ^{129}Xe present as an impurity in the plasma gas *via* a charge transfer reaction that has limited impact on ^{129}I . The additional mass filter improved stable ^{127}I tailing removal, as well as in cell oxide polyatomic formation, most notably $^{97}\text{Mo}^{16}\text{O}_2$. Recent work has also shown that carbon-based matrix modification considerably improved instrument sensitivity, helping to overcome the high first ionisation energy of iodine.⁴⁷

Neptunium-237 is a long-lived radionuclide that has been measured using a range of ICP-MS designs.^{2,3,48,49} The most significant interference is tailing from ^{238}U , which can be removed by offline chemical separation.^{50,51} Operating in MS/MS mode, ^{237}Np detection is possible even at ^{238}U concentrations of $10 \text{ } \mu\text{g g}^{-1}$ (Fig. 4), whilst there was an increase in background at $m/z = 237$ at ^{238}U concentrations of 5 ng g^{-1} and above in Single Quad mode. This instrument setup has been effectively used for measuring ^{237}Np in spiked uranium samples⁵² and sediment samples following chemical separation,⁵³ with the latter achieving a detection limit of 25.0 pg g^{-1} ($6.5 \times 10^{-4} \text{ Bq g}^{-1}$).

Plutonium-239 has been extensively measured by ICP-MS, often in combination with ^{240}Pu to determine the source of nuclear contamination through the difference in $^{239}\text{Pu}/^{240}\text{Pu}$ isotopic ratio values.^{54–56} The ICP-MS/MS setup has been shown to reduce the reliance on offline chemical separation from ^{238}U ,

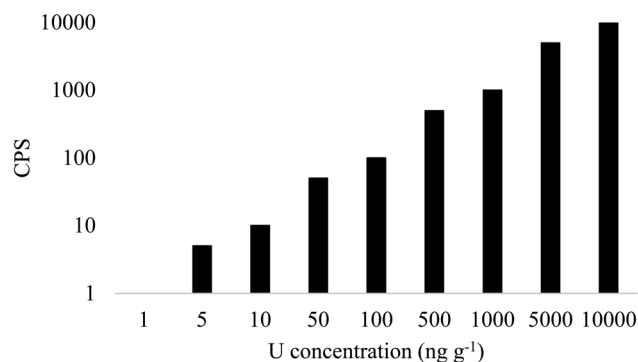


Fig. 4 Signal at $m/z = 237$ with increasing concentration of ^{238}U in Single Quad mode. 0 CPS were measured in MS/MS mode.



Table 5 A summary of the various gas modes used to measure Tc sensitivity and the background contribution of Ru and Mo in these modes, with the selected method shown in bold

Mode	Q1	Q2	CPS per Bq g ⁻¹ Tc	10 ng g ⁻¹ Ru signal (CPS)	1 µg g ⁻¹ Mo signal (CPS)
MS/MS no gas	99	99	245 000	200 000	100
MS/MS O ₂ (on mass)	99	99	126 500	111 000	200
MS/MS O ₂ (single oxide)	99	115	24 500	15 000	35
MS/MS O₂ (double oxide)	99	131	25 000	160	5
MS/MS NH ₃	99	185	3000	40	120

which otherwise interferes *via* tailing and formation of poly-atomic $^{238}\text{U}^1\text{H}$.^{12,13} The Agilent 8800 used in this study has a maximum m/z value of 260, limiting the number of cell products that can be formed in NH₃ and O₂ mode. Recently developed ICP-MS/MS instruments can measure at higher m/z values, and this has been shown to be beneficial for actinide measurement and separation through double oxide formation.⁵⁷

In NH₃ mode at a flow rate of 3 mL min⁻¹, the majority (96%) of the Pu signal remained on mass. By comparison, only 18% of the total ^{238}U signal remained on mass, with the remainder measured as U(NH) and U(NH₂). When ^{239}Pu was measured on mass in NH₃ mode, a $^{238}\text{U}^1\text{H}$ interference was still present, but was reduced by an order of magnitude compared to MS/MS no gas mode (Fig. 5). At an O₂ flow rate of 0.3 mL min⁻¹, >95% of the U and Pu was shifted to an oxide. Compared to MS/MS no-gas and NH₃ mode, the interference from $^{238}\text{U}^1\text{H}$ is significantly reduced when measuring Pu as $^{239}\text{Pu}^{16}\text{O}$. This is a result of $^{238}\text{U}^1\text{H}$ being converted to $^{238}\text{U}^{16}\text{O}$ in the reaction cell, with limited formation of $^{238}\text{U}^{16}\text{O}^1\text{H}$ (Fig. 5). At a ^{238}U concentration of 10 µg g⁻¹, the signal at $m/z = 239$ was 45 600 CPS in MS/MS no gas, 5100 CPS in MS/MS NH₃, and 165 CPS in MS/MS O₂ mode when measuring Pu as $^{239}\text{Pu}^{16}\text{O}$.

Increasing the O₂ gas flow rate reduced the $^{238}\text{U}^{16}\text{O}^1\text{H}$ formation, at the expense of $^{239}\text{Pu}^{16}\text{O}$ sensitivity (Fig. 6). The optimal flow rate was determined to be 0.4 mL min⁻¹, with the background at $m/z = 255$ (*i.e.* $^{239}\text{Pu}^{16}\text{O}$) from a 10 µg g⁻¹ ^{238}U solution of 45 CPS, compared to 165 at 0.3 mL min⁻¹. Under the

optimised conditions, the instrument LOD for ^{239}Pu in this study was 0.27 mBq g⁻¹ (0.12 pg g⁻¹).

3.2. Development of a combined procedure for multiple radionuclides

The instrument software allows the setting of up to eight modes within a single run. The instrument parameters for seven radionuclides along with a mode for stable elements is shown in Table 6. A switching time of 25 seconds was programmed between each mode to allow the instrument settings to adjust and settle before measurement. The total analysis time was approximately seven minutes per sample, with an additional wash time of 5 minutes between each sample. A mixed $^9\text{Be}/^{115}\text{In}/^{209}\text{Bi}$ (50 ng g⁻¹) internal standard was measured within each mode to account for instrument drift, which was connected *via* the dedicated internal standard line in the sample introduction system, preventing the need to individually spike samples.

Iodine-129 is included in Table 6, however, because it must be prepared in alkaline solution due to its volatility, it could not be included in the same run. Instead, following the measurement of other radionuclides, multiple washes were added to the procedure, which proceeded automatically after the end of the previous run: (1) 10 minutes in 0.3 M HNO₃, (2) 20 minutes in deionised water to wash acid out of the instrument and (3) 20 minutes conditioning in 0.001 NaOH. The ^{129}I procedure then started automatically. A 10 ng g⁻¹ Te standard was monitored at

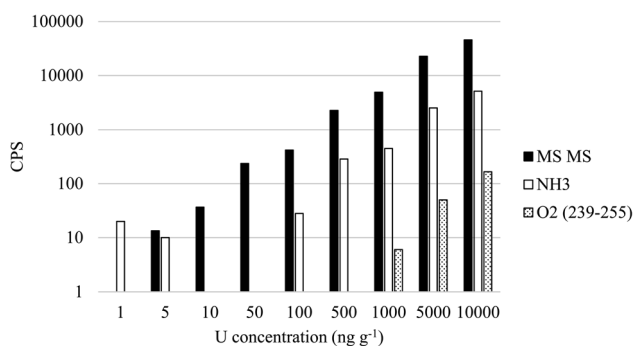


Fig. 5 Impact of ^{238}U concentration on tailing and hydride formation at $m/z = 239$ in MS/MS mode, NH₃ mode and O₂ mode (Pu measured as $^{239}\text{Pu}^{16}\text{O}$).

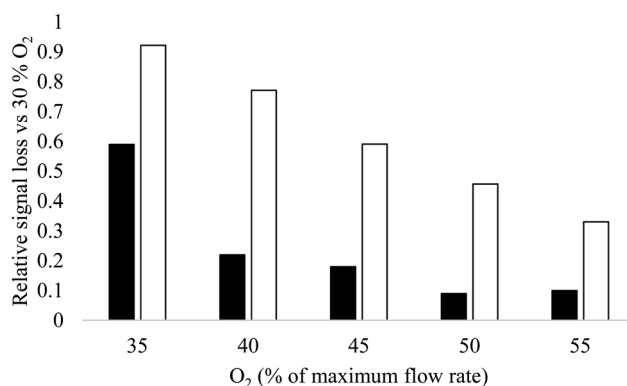


Fig. 6 Impact of O₂ flow rate on $^{239}\text{Pu}^{16}\text{O}$ sensitivity (no fill) and $^{238}\text{U}^{16}\text{O}^1\text{H}$ (filled in) interference formation for a 10 µg g⁻¹ ^{238}U solution relative to standard tune setting of 30% O₂ (0.3 mL min⁻¹).



Table 6 Summary of instrument setup for simultaneous measurement of multiple radionuclides

Parameter	Stable	⁶³ Ni	⁹⁰ Sr	⁹³ Zr	⁹⁹ Tc	¹²⁹ I	²³⁷ Np	²³⁹ Pu
Mode	MS/MS							
Q1–Q2	Various	63–114	90–90	93–195	99–131	129–129	237–237	239–255
RF (W)					1550			
Carrier gas (L min ^{−1})					0.65			
Dilution gas (L min ^{−1})					0.35			
Extract 1 (V)					0			
Extract 2 (V)					−175			
H ₂ (mL min ^{−1})		3.00		3.00				
He (mL min ^{−1})	4.00	1.00		2.00				
O ₂ (mL min ^{−1})			0.40		0.30	0.55		0.40
NH ₃ (mL min ^{−1})		1.00		0.15				
Energy discrimination (V)	5.0	−13.0	−18.0	−9.0	−7.0	−6.0		−7.0
Octopole bias (V)	−18.0	−4.5	0.0	−2.8	−5.0	−2.0		−5.0
Internal standard	¹¹⁵ In/ ²⁰⁹ Bi	¹¹⁵ In	¹¹⁵ In	¹¹⁵ In	¹¹⁵ In	¹³⁰ Te	²⁰⁹ Bi	²⁰⁹ Bi

$m/z = 130$, which was manually spiked into the solutions rather than using the internal standard line.⁴⁷

The 'stable' mode in Table 6 operates in MS/MS mode with He collision gas at a flow rate of 4 mL min^{−1}. It is therefore suitable for several radionuclides that do not suffer from isobaric interferences. Polyatomic interferences should be suppressed by the collision gas, whilst tailing removal is improved by operating in MS/MS mode. This mode is considered suitable for ²²⁶Ra, ²³¹Pa, ²³²Th, ²³⁴U, ²³⁵U, ²³⁸U, ²⁴¹Am and ²⁴³Am. Neptunium-237 could also be run in this mode, as the long half life means low detection limits can still be achieved even following signal suppression from the use of He. This approach also enables an additional mode to be used, with procedures published elsewhere for ICP-MS/MS measurement of ⁴¹Ca,⁵⁸ ¹⁵¹Sm⁵⁹ and ²³⁶U.⁹ It should also be noted that the procedure developed for ²³⁹Pu is also applicable to ²⁴⁰Pu.

3.3. Testing of the combined procedure

To test the potential of the combined procedure, several matrices were measured (groundwater, aqueous waste, air filters, soil, sediment and concrete). In all cases, no offline chemical separation was performed. Air filters were digested using a microwave, whilst soil, sediment and concrete samples were digested using lithium borate fusion.

For each sample type, matrix-matched calibration standards using multi-element stable standard solutions and radionuclide standard solutions were produced. The calibration curves were used to determine the method LOD, calculated as the equivalent concentration of three times the standard deviation of the blank in unspiked samples. Each sample run consisted of 10 replicates and 100 sweeps per replicate.

The concentration of a range of stable elements spanned several orders of magnitude (Table 7), indicating the range of matrix compositions of the samples measured. The values shown are the concentrations in the original samples, factoring in corrections for sample dilution where this was applied. It must be noted that a higher dilution factor was used for solid samples digested using borate fusion prior to measurement,

resulting in a much lower concentration in the samples measured compared to in the starting material. Amongst the stable elements tested were those that represent isobaric interferences for radionuclides of interest to this study, including ⁹⁰Zr (⁹⁰Sr), ⁶³Cu (⁶³Ni), ⁹³Nb (⁹³Zr) and ⁹⁹Ru (⁹⁹Tc), as well as tailing interferences including ⁸⁸Sr (⁹⁰Sr), ⁹⁸Mo (⁹⁹Tc) and ²³⁸U (²³⁷Np and ²³⁹Pu).

A mixed 50 ng g^{−1} Be/In/Bi internal standard was used to assess instrument drift and any suppression of the signal and reduced ion transmission due to solid sample deposition on the interface cones over time.

Method detection limits for each of the radionuclides of interest were determined (calculated from the equivalent concentration of three times the standard deviation of the blanks in unspiked samples) in their optimised mode, compared to the instrument LOD for interference-free samples (Fig. 7).

The decontamination factor achieved by the collision/reaction cell was a key consideration. This was calculated for

Table 7 Stable element composition of samples tested

Element	Concentration range ^a (ng g ^{−1})
Co	<1 to 3.7 × 10 ³
Ni	<1 to 7.1 × 10 ³
Cu	2 to 4.4 × 10 ³
Zn	5 to 1.7 × 10 ⁴
Sr	2 to 1.9 × 10 ⁴
Y	<1 to 1.6 × 10 ³
Zr	1 to 4.4 × 10 ⁴
Nb	1–470
Mo	2–340
Ru	<1–35
Cs	<1–330
Ba	20 to 5.7 × 10 ⁴
Th	<1–700
U	2–1000

^a Corrected to concentration per unit mass of the starting sample.



each sample matrix by dividing the CPS at the interfering m/z value compared by the CPS at the analyte m/z value in each optimal instrument mode. For example, for ^{90}Sr , the ^{90}Zr decontamination factor was calculated as the CPS at $m/z = 106$ (where ^{90}Zr preferentially forms $^{90}\text{Zr}^{16}\text{O}$) to the CPS at $m/z = 90$ (where ^{90}Sr is expected). To ensure that the interference was the result of an isobaric interference, where possible an isotope of the same element as the isobar was also measured (e.g. ^{91}Zr for ^{90}Zr) and the ratio between the counts compared to natural ratios. This was not possible for monoisotopic ^{93}Nb , however, the maximum Zr concentration measured (880 ng g $^{-1}$ in sediment) was not high enough to result in ^{92}Zr tailing in MS/MS mode, whilst there was no evidence of polyatomic $^{92}\text{Zr}^{1}\text{H}$ formation following a mass shift of $m/z +195$. Therefore, the signal at $m/z = 93$ was expected to be the result of isobaric ^{93}Nb .

Across all samples tested for ^{63}Ni , the average cell decontamination factor of isobaric ^{63}Cu using $\text{NH}_3 + \text{H}_2$ was 6.9×10^2 . For ^{63}Ni standards in the optimum instrument mode (measured as $^{63}\text{Ni}(\text{NH}_3)_3$), the target was a background of <5 CPS. This compared to a range of 7–182 CPS (average 38 CPS) in groundwater samples, 123–1560 CPS (average 940 CPS) for air filters, and 108–701 CPS (average 360 CPS) across the solid samples tested. The instrument LOD was calculated as 0.50 Bq g $^{-1}$ (0.24 pg g $^{-1}$), increasing to an average of 25.6 Bq g $^{-1}$ (12.0 pg g $^{-1}$) in aqueous waste samples, 30.7 Bq g $^{-1}$ (14.4 pg g $^{-1}$) in groundwaters, 128.5 (60.4 pg g $^{-1}$) Bq g $^{-1}$ across the solid samples tested and 331.2 Bq g $^{-1}$ (155.7 pg g $^{-1}$) in air filter samples.

The relatively short half life of ^{63}Ni (1 Bq g $^{-1}$ is equivalent of 0.5 pg g $^{-1}$) results in both a lower sensitivity and higher impact of interferences relative to the same activity concentration of longer-lived radionuclides. The highest isobaric ^{63}Cu concentration measured (4.4 ng g $^{-1}$) in final samples was measured in air filters, which produced the highest calculated detection limit of the samples measured. Whilst the reaction cell does achieve some decontamination of interferences, even relatively low ^{63}Cu concentrations will contribute to the ^{63}Ni signal. For air filters and groundwater samples in particular, there was a significant range in instrument backgrounds measured. One groundwater sample had a background in the optimal setup of 182 CPS, compared to the next highest value of 49 CPS. If this higher background sample was not included, the method detection limit across the samples measured will have been 9.0 Bq g $^{-1}$ (4.2 pg g $^{-1}$), compared to 30.7 Bq g $^{-1}$ (14.4 pg g $^{-1}$). It was

a similar case for air filter samples, with three samples having a background of > 900 CPS, compared to 123 CPS for the fourth air filter measured. In both cases, this shows the importance of measuring a range of sample matrices when determining the application of this method.

The results for ^{90}Sr followed a similar trend to those for ^{63}Ni and was the shortest-lived radionuclide in this study. In agreement with previous studies, O_2 was an effective reaction gas in shifting ^{90}Zr to $^{90}\text{Zr}^{16}\text{O}$, whilst the majority of the ^{90}Sr signal remained on mass. The average cell decontamination factor of ^{90}Zr across the samples tested was 6.0×10^2 . The instrument background in the optimised setup was <5 CPS. A similar value was achieved for groundwater samples (maximum 8 CPS), increasing to 9–56 CPS (average 40 CPS) in air filter samples and a significantly higher average value of 1880 CPS (168–2960 CPS) across the solid samples tested.

The relatively short half life for ^{90}Sr meant it had the highest instrument LOD of any radionuclide in this study, with a calculated value of 1.0 Bq g $^{-1}$ (0.2 pg g $^{-1}$). This also meant that any increase in background at $m/z = 90$ had a more significant impact on the detection limit compared to the other radionuclides investigated. The low background across groundwater samples resulted in a method LOD that matched the instrument LOD of 1.0 Bq g $^{-1}$ (0.2 pg g $^{-1}$), increasing to 3.2 Bq g $^{-1}$ (4.2 pg g $^{-1}$) in air filters, 90.0 Bq g $^{-1}$ (17.6 pg g $^{-1}$) in aqueous waste samples and 173.9 Bq g $^{-1}$ (34.1 pg g $^{-1}$) across the solid samples tested. The increase in background is primarily from isobaric ^{90}Zr . Despite the decontamination achieved by the reaction cell, concentrations of up to 880 ng g $^{-1}$ were measured that will not be completely removed by reaction cell separation alone and will contribute significantly to the background. The highest stable ^{88}Sr concentration of 380 ng g $^{-1}$ is not expected to result in a tailing interference when measured in MS/MS mode.

For ^{93}Zr , in instrument blank solutions, the background was 0 CPS, with a background of <10 CPS across all samples tested, suggesting the significant mass shift of 102 from $m/z = 93$ to $m/z = 195$ (i.e. $^{93}\text{Zr}(\text{NH}_3)_6$) effectively reduces interferences, primarily from ^{93}Nb). The method LOD was on the order of 1×10^{-4} Bq g $^{-1}$ (1.1 pg g $^{-1}$), in agreement with those achieved in previous studies.^{14,15}

Technetium-99 used O_2 cell gas for interference removal. The background for samples tested was not significantly different to the instrument background (<10 CPS), with the instrument and method LOD values of 3.0×10^{-4} Bq g $^{-1}$ (0.5 pg g $^{-1}$) and $3.1 \times$

Table 8 Instrument and method limit of detection for radionuclides of interest

Radionuclide	Instrument LOD (Bq g $^{-1}$, pg g $^{-1}$)	Method LOD (Bq g $^{-1}$, pg g $^{-1}$)
^{63}Ni	0.5 (0.3)	25.6 (12.1)–331.2 (155.7)
^{90}Sr	1.0 (0.2)	1.0 (0.2)–173.9 (34.1)
^{93}Zr	1.3×10^{-5} (0.1)	1.7×10^{-4} (2.2)
^{99}Tc	3.0×10^{-4} (0.5)	3.1×10^{-4} (0.6)
$^{129}\text{I}^a$	8.1×10^{-5} (5.2)	8.6×10^{-5} (5.1)
^{237}Np	1.0×10^{-5} (0.4)	1.1×10^{-4} (4.2)
^{239}Pu	1.6×10^{-4} (0.07)	1.6×10^{-3} (0.7)

^a Iodine-129 only measured in aqueous samples



10^{-4} Bq g $^{-1}$ (0.6 pg g $^{-1}$). Direct measurement as $^{99}\text{Tc}^{16}\text{O}_2$ was possible in the samples measured due to the relatively low Ru (isobaric) and Mo (tailing and polyatomic $^{98}\text{Mo}^{1}\text{H}$) concentrations. A Ru concentration of 10 ng g $^{-1}$ increased the background at $m/z = 131$ by approximately 160 CPS, compared to 25 000 CPS for a 1 Bq g $^{-1}$ ^{99}Tc solution, suggesting that samples containing higher Ru concentrations will require offline chemical separation in combination with reaction cell separation. The maximum Mo concentration of 110 ng g $^{-1}$ did not significantly contribute to the instrument background (Table 8).

Iodine-129 was measured on-mass, using O_2 reaction gas to suppress the background from isobaric ^{129}Xe present as an impurity in the Ar plasma gas, in agreement with previous studies.^{44–46} Operating in MS/MS mode effectively removed any potential interference from ^{129}I tailing. MS/MS mode will not remove $^{127}\text{I}^{1}\text{H}_2$ formed in the plasma, but this can be suppressed by operating with O_2 reaction gas. Polyatomic $^{97}\text{Mo}^{16}\text{O}_2$ has been recorded as interfering with the background at $m/z = 129$ at Mo concentrations of 500 ng g $^{-1}$ and above,⁴⁷ which is higher than the maximum value from samples in this study of 110 ng g $^{-1}$. Iodine-129 was only measured in aqueous samples, as its volatile nature means borate fusion dissolution is not an appropriate sample preparation technique. As with ^{99}Tc , the instrument and method LOD calculated were very similar (8.1×10^{-5} Bq g $^{-1}$ (5.2 pg g $^{-1}$) and 8.6×10^{-5} Bq g $^{-1}$ (5.1 pg g $^{-1}$), respectively).

Neptunium-237 was measured on mass in MS/MS mode, with a background of 0 CPS in the instrument and all method blank samples. This showed the MS/MS setup to effectively remove ^{238}U tailing in the samples tested (with ^{238}U concentrations up to 1000 ng g $^{-1}$), removing the need for offline chemical separation. The method LOD was on the order of 1.1×10^{-4} Bq g $^{-1}$ (4.2 pg g $^{-1}$). The ^{238}U tailing removal was also beneficial for ^{239}Pu measurement, whilst measurement of ^{239}Pu as $^{239}\text{Pu}^{16}\text{O}$ minimised the impact of $^{238}\text{U}^{1}\text{H}$ through effective

conversion to $^{238}\text{U}^{16}\text{O}$. The background was <10 CPS across the samples measured, with a method LOD calculated as 1.6×10^{-3} Bq g $^{-1}$ (0.7 pg g $^{-1}$).

Regulatory limits vary between organisations and countries depending on the nature of the sample being measured. The range of samples measured are a good indicator of whether the method developed for simultaneous radionuclide measurement is applicable for end users as a rapid approach for assessing sample composition. The detection limits calculated were compared to several regulatory limits related to drinking water, environmental permitting, radiation protection and waste exemption.^{60–63} For ^{93}Zr , ^{99}Tc , ^{129}I and ^{237}Np , the detection limits are lower than the regulatory limits (Fig. 7), whilst for ^{239}Pu , the detection limit (1.6×10^{-3} Bq g $^{-1}$) was lower than all limits other than the WHO drinking water limit (1 mBq mL $^{-1}$).

As expected, radionuclides with a shorter half life are less likely to be candidates for direct low-level measurement compared to long-lived radionuclides. Despite the relatively high detection limits for ^{63}Ni , (25.6–331.2 Bq g $^{-1}$ (12.1–155.7 pg g $^{-1}$)), this value is lower than some the regulatory limits tested, meaning that direct measurement is feasible for some applications. For ^{90}Sr , a highly important radionuclide with regards to decommissioning, waste characterisation and public safety, the detection limit calculated is generally higher than the regulatory limits. It is therefore necessary that measurement is preceded by chemical separation and pre-concentration prior to measurement. This is the approach that has been taken in previous studies, with reduced procedural times achieved using online separation, for example using sequential injection.^{5,43,44} Chemical separation would also enable decay counting measurement of both ^{63}Ni and ^{90}Sr by LSC to check the agreement between decay counting and mass spectrometric techniques. Additionally, other sample dissolution techniques that can handle higher starting sample masses compared to borate fusion (such as open vessel acid leaching) have not been

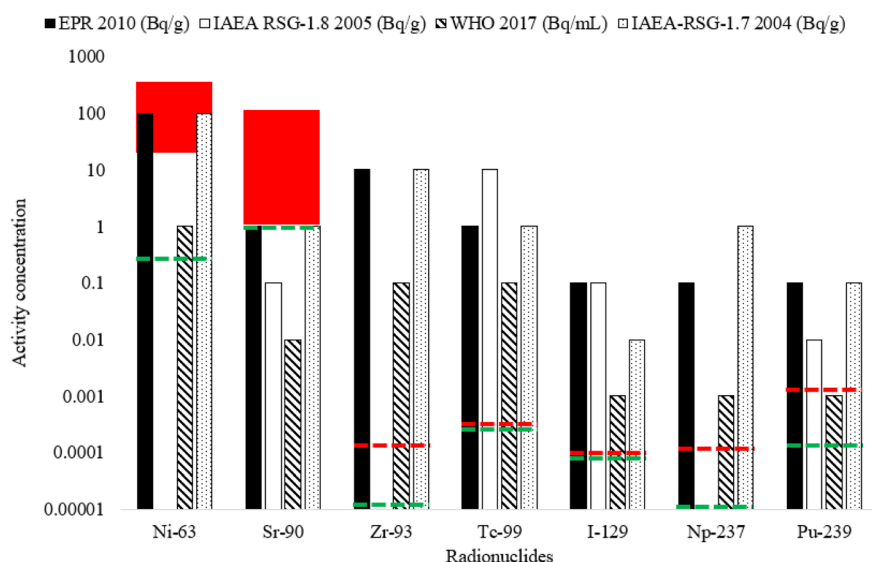


Fig. 7 Instrument detection limit (dashed green line) and method detection limit (dashed red line) for radionuclides of interest compared to multiple regulations. The solid red area for ^{63}Ni and ^{90}Sr shows the range in method LOD's calculated.



considered, which may be beneficial for relatively short-lived radionuclides.¹³

Preliminary results from stable Ni and Sr standards using an Agilent 8900 suggests the instrument sensitivity and cell-based interference removal is considerably improved compared to the previous generation Agilent 8800 used in this study, which could be particularly beneficial for shorter-lived radionuclides. In the case of Sr, the sensitivity was approximately five times higher using the newer instrument, with more efficient formation of $^{90}\text{Zr}^{16}\text{O}$ and no change in $^{90}\text{Sr}^{16}\text{O}$ formation. Compared to the Agilent 8800 used in this study, the updated Agilent 8900 has a new interface vacuum stage for improved ion transmission and an updated collision reaction cell with axial acceleration, which further improves sensitivity and reaction cell efficiency, respectively.

The results show the ability to directly measure multiple radionuclides without prior separation, which minimises the analyst time, secondary waste produced, loss of analyte during the procedure, and the need for tracer addition, which all offer economic benefits to the end user, and improves sample throughput. It should be noted that the radionuclides in Table 8 are an example of the combination that can be tested, and the user can select up to eight modes depending on the target radionuclides of interest. Initial data suggests that additional radionuclides can be included in the combined procedure, specifically ^{36}Cl and ^{93}Mo .²⁵

In this study, several O_2 modes have been used that have been customised for individual radionuclides, but it may be possible to develop a single mode that would be applicable to ^{90}Sr , ^{99}Tc , ^{151}Sm and ^{239}Pu . Such an approach is likely to reduce sensitivity for all radionuclides compared to the individually tailored method used in this study, which would have a more significant effect on shorter-lived radionuclides. Again, the approach used ultimately depends on the number of radionuclides that must be measured, and the limits of detection required.

The instrument used in this study has four gas lines-dedicated H_2 and He , one non-corrosive line (O_2) and one corrosive line (NH_3). The use of other gases was not considered, for example $^{135}\text{Cs}/^{137}\text{Cs}$ has been effectively measured by ICP-MS/MS using N_2O as a reaction gas to shift isobaric ^{135}Ba and ^{137}Ba to oxides. Alternative gases could potentially enable detection of radionuclides that to date have not been measured by ICP-MS, such as ^{59}Ni . Additionally, the instrument used in this study requires the NH_3 to be balanced in at least 90% He to protect the cell. Other ICP-MS/MS instrument designs can tolerate higher NH_3 concentrations, which may offer more efficient cell-based interference separation and expand the number of radionuclides measurable.

4. Conclusions and future work

The capabilities of ICP-MS/MS have been tested for simultaneous measurement of multiple radionuclides in several sample matrices. Methods have been developed for ^{63}Ni , ^{90}Sr , ^{93}Zr , ^{99}Tc , ^{129}I , ^{237}Np and ^{239}Pu , which offers a good assessment of instrument capabilities for radionuclide measurement. In all

cases, the MS/MS configuration and collision/reaction cell have been customised to offer good sensitivity combined with enhanced removal of isobaric, polyatomic and tailing interferences. The final procedure developed is capable of simultaneously measuring all radionuclides of interest and stable element composition. This approach can be extended further to include other radionuclides, including ^{226}Ra , ^{238}U and ^{241}Am . For longer-lived radionuclides (e.g. ^{99}Tc , ^{129}I , ^{237}Np and ^{239}Pu), method detection limits in the mBq g^{-1} region was achievable, meaning that low-level direct measurement without prior separation is possible. For shorter-lived radionuclides such as ^{63}Ni and ^{90}Sr , the method LOD was notably higher than the instrument LOD due to the relatively high impact of stable interferences compared to longer-lived radionuclides. This may necessitate offline chemical separation prior to measurement depending on the target detection limits.

The procedure developed demonstrates the capabilities of ICP-MS/MS for direct measurement of radionuclides without prior treatment, as well as showing the amount of information that can be generated about a sample in a single measurement. There are additional radionuclides that could potentially benefit from the high sample throughput and improved interference separation of ICP-MS/MS, for example ^{59}Ni . Additionally, there are reaction gases not tested in this study that may further improve interference removal or expand the number of radionuclides measurable, such as N_2O for measurement of $^{135}\text{Cs}/^{137}\text{Cs}$. There is also the possibility of measuring isotopic ratios to determine the source of contamination, for example $^{127}\text{I}/^{129}\text{I}$, $^{135}\text{Cs}/^{137}\text{Cs}$, and $^{239}\text{Pu}/^{240}\text{Pu}$.

Conflicts of interest

There are no conflicts to declare.

Acknowledgements

NPL authors thank Sellafield Ltd. for provision of samples and funding that led to the initial development of this procedure. NPL also acknowledge funding from the National Measurement System by the Department of Business, Energy and Industrial Strategy. The iodine-129 method was developed as part of a joint funded PhD project between the University of Southampton and NPL. The work on technetium-99 was undertaken through a placement at NPL as part of a Royal Holloway MSc in Environmental Diagnosis and Management.

References

- 1 D. Larivière, V. F. Taylor, R. D. Evans and R. J. Cornett, Radionuclide determination in environmental samples by inductively coupled plasma mass spectrometry, *Spectrochim. Acta, Part B*, 2006, **61**, 877–904.
- 2 X. Hou and P. Roos, Critical comparison of radiometric and mass spectrometric methods for the determination of radionuclides in environmental, biological and nuclear waste samples, *Anal. Chim. Acta*, 2008, **608**, 105–139.



- 3 I. W. Croudace, B. C. Russell and P. E. Warwick, Plasma source mass spectrometry for radioactive waste characterisation in support of nuclear decommissioning: a review, *J. Anal. At. Spectrom.*, 2017, **32**, 494–526.
- 4 B. Russell, M. García-Miranda and P. Ivanov, Development of an optimised method for analysis of ^{90}Sr in decommissioning wastes by triple quadrupole inductively coupled plasma mass spectrometry, *Appl. Radiat. Isot.*, 2017, **126**, 35–39.
- 5 J. Tomita and E. Takeuchi, Rapid analytical method of ^{90}Sr in urine sample: Rapid separation of Sr by phosphate co-precipitation and extraction chromatography, followed by determination by triple quadrupole inductively coupled plasma mass spectrometry (ICP-MS/MS), *Appl. Radiat. Isot.*, 2019, **150**, 103–109.
- 6 Y. Shikamori, K. Nakano, N. Sugiyama and S. Kakuta, *The ultratrace determination of iodine 129 using the Agilent 8800 Triple Quadrupole ICP-MS in MS/MS mode*, Agilent Technical Note, 2017, <https://hpst.cz/sites/default/files/oldfiles/5991-0321en-ultratrace-determination-iodine-129-using-agilent-8800-triple-quadrupole-icp-ms-ms.pdf>, accessed 26/09/2022.
- 7 I. J. Arnquist, G. C. Eiden, J. Lewis, C. D. Coath, H. Wehrs, J. Schwieters and T. Elliot, *The Right Tool for the I-129 Job: Can Triple Quad ICPMS or Collision Cell MC-ICPMS (Proteus) Address Limitations of AMS and TIMS? Goldschmidt Conference*, Boston, 2018.
- 8 J. Zheng, K. Tagami and W. Bu, $^{135}\text{Cs}/^{137}\text{Cs}$ isotopic ratio as a new tracer of radiocesium released from the Fukushima nuclear accident, *Environ. Sci. Technol.*, 2014, **48**(10), 5433–5438.
- 9 M. Tanimizu, N. Sugiyama, E. Ponzevera and G. Bayon, Determination of ultra-low $^{236}\text{U}/^{238}\text{U}$ isotope ratios by tandem quadrupole ICP-MS/MS, *J. Anal. At. Spectrom.*, 2013, **28**, 1372–1376.
- 10 E. M. van Es, B. C. Russell, P. Ivanov and D. Read, Development of a method for rapid analysis of Ra-226 in groundwater and discharge water samples by ICP-QQQ-MS, *Appl. Radiat. Isot.*, 2017, **126**, 31–34.
- 11 C. Dalencourt, A. Michaud, A. Habibi, A. Le Blanc and D. Larivière, Rapid, versatile and sensitive method for the quantification of radium in environmental samples through cationic extraction and inductively coupled plasma mass spectrometry, *J. Anal. At. Spectrom.*, 2018, **33**, 1031–1040.
- 12 P. E. Warwick, B. C. Russell, I. W. Croudace and Ž. Zacharuskas, Evaluation of inductively coupled plasma tandem mass spectrometry for radionuclide assay in nuclear waste characterisation, *J. Anal. At. Spectrom.*, 2019, **34**, 1810–1821.
- 13 M. A. Amr, A. F. I. Helal, A. T. Al-Kinani and P. Balakrishnan, Ultra-trace determination of ^{90}Sr , ^{137}Cs , ^{238}Pu , ^{239}Pu , and ^{240}Pu by triple quadrupole collision/reaction cell-ICP-MS/MS: Establishing a baseline for global fallout in Qatar soil and sediments, *J. Environ. Radioact.*, 2016, **153**, 73–87.
- 14 P. Petrov, B. Russell, D. N. Douglas and H. Goenaga-Infante, Interference-free determination of sub ng kg $^{-1}$ levels of long-lived ^{93}Zr in the presence of high concentrations ($\mu\text{g kg}^{-1}$) of ^{93}Mo and ^{93}Nb using ICP-MS/MS, *Anal. Bioanal. Chem.*, 2018, **410**, 1029–1037.
- 15 H. Thompkins, B. Russell and S. Goddard, *Direct Analysis of Zirconium-93 in Nuclear Site Decommissioning Samples by ICP-QQQ*, Agilent Application Note, 2020, pp. 1–5, https://www.agilent.com/cs/library/applications/application_zr-93_icp-qqq_8800_8900_5994-1532en_us-agilent.pdf, accessed 26/09/2022.
- 16 S. Goddard, R. J. Brown, D. Butterfield, E. McGhee, C. Robins, A. Brown, S. Beccaceci, A. Lilley, C. Bradshaw and S. Brennan, *Annual Report for 2014 on the UK Heavy Metals Monitoring Network*, Queen's Printer and Controller of HMSO, 2015.
- 17 I. Croudace, P. Warwick, R. Taylor and S. Dee, Rapid procedure for plutonium and uranium determination in soils using a borate fusion followed by ion-exchange and extraction chromatography, *Anal. Chim. Acta*, 1998, **371**(2–3), 217–225.
- 18 E. Braysher, B. Russell, S. Woods, M. Garcia-Miranda, P. Ivanov and D. Read, Complete dissolution of solid matrices using automated borate fusion in support of nuclear decommissioning and production of reference materials, *J. Radioanal. Nucl. Chem.*, 2019, **321**, 183–196.
- 19 Eichrom Technologies, *Nickel-63/59 in water*, Eichrom Analytical Procedure, 2014, https://www.eichrom.com/wp-content/uploads/2018/02/niw01-13_ni-water.pdf, accessed 26/09/22.
- 20 E. Holm, P. Roos and B. Skwarzec, Radioanalytical studies of fallout ^{63}Ni , *Int. J. Radiat. Appl. Instrum., Part A*, 1992, **43**(1–2), 371–376.
- 21 O. Rosskopfová, M. Galamboš and P. Rajec, Determination of ^{63}Ni in the low level solid radioactive waste, *J. Radioanal. Nucl. Chem.*, 2011, **289**, 251–256.
- 22 P. E. Warwick and I. W. Croudace, Isolation and quantification of ^{55}Fe and ^{63}Ni in reactor effluents using extraction chromatography and liquid scintillation analysis, *Anal. Chim. Acta*, 2006, **567**(2), 277–285.
- 23 X. Hou, L. F. Østergaard and S. P. Nielsen, Determination of ^{63}Ni and ^{55}Fe in nuclear waste samples using radiochemical separation and liquid scintillation counting, *Anal. Chim. Acta*, 2005, **1–2**, 297–307.
- 24 C. Gascó, M. C. Heras, A. Suanes, A. Alvarez, N. Navarro and A. Alvarez, *The difficulties of measuring ^{55}Fe and ^{63}Ni in environmental samples*, IAEA International Nuclear Information System, 2008, vol. 41, issue 1, pp. 1–10.
- 25 B. Russell, S. L. Goddard, H. Mohamud, O. Pearson, Y. Zhang, H. Thompkins and R. J. C. Brown, Applications of hydrogen as a collision and reaction cell gas for enhanced measurement capability applied to low level stable and radioactive isotope detection using ICP-MS/MS, *J. Anal. At. Spectrom.*, 2021, **36**, 2704–2714.
- 26 F. Wigley, P. E. Warwick, I. W. Croudace, J. Caborn and A. L. Sanchez, Optimised method for the routine determination of Technetium-99 in environmental samples by liquid scintillation counting, *Anal. Chim. Acta*, 1999, **380**(1), 73–82.



- 27 K. Shi, X. Hou, P. Roos and W. Wu, Determination of technetium-99 in environmental samples: A review, *Anal. Chim. Acta*, 2012, **709**, 1–20.
- 28 J. L. Más, K. Tagami and S. Uchida, Method for the detection of Tc in seaweed samples coupling the use of Re as a chemical tracer and isotope dilution inductively coupled plasma mass spectrometry, *Anal. Chim. Acta*, 2004, **509**(1), 83–88.
- 29 J. L. Más, M. Garcia-Leon and J. P. Bolivar, ⁹⁹Tc atom counting by quadrupole ICP-MS. Optimisation of the instrumental response, *Nucl. Instrum.*, 2002, **484**(1–3), 660–667.
- 30 K. H. Chung, S. D. Choi, G. S. Choi and M. J. Kang, Design and performance of an automated radionuclide separator: Its application on the determination of ⁹⁹Tc in groundwater, *Appl. Radiat. Isot.*, 2013, **81**, 57–61.
- 31 Q. Chen, H. Dahlgard, H. J. M. Hansen and A. Aarkrog, Determination of ⁹⁹Tc in environmental samples by anion exchange and liquid-liquid extraction at controlled valency, *Anal. Chim. Acta*, 1990, **228**, 163–167.
- 32 R. Seki and M. Kondo, An improved method for technetium determination in environmental samples, *J. Radioanal. Nucl. Chem.*, 2005, **263**, 393–398.
- 33 C. Dale, P. E. Warwick and I. W. Croudace, An optimized method for Technetium-99 determination in Low-Level waste by extraction into Tri-n-octylamine, *Radioact. Radiochem.*, 1996, **7**, 23–31.
- 34 A. E. Eroglu, C. W. McLeod, K. S. Leonard and D. McCubbin, Determination of technetium in sea-water using ion exchange and inductively coupled plasma mass spectrometry with ultrasonic nebulisation, *J. Anal. At. Spectrom.*, 1998, **13**, 875–878.
- 35 K. Tagami and S. Uchida, Comparison of the TEVA-Spec resin and liquid-liquid extraction methods for the separation of technetium in soil samples, *J. Radioanal. Nucl. Chem.*, 1999, **239**, 643–648.
- 36 N. Guérin, R. Riopel, S. Kramer-Tremblay, N. de Silva, J. Cornett and X. Dai, Determination of ⁹⁹Tc in fresh water using TRU resin by ICP-MS, *Anal. Chim. Acta*, 2017, **988**, 114–120.
- 37 L. S. Chen, T. H. Wang, Y. K. Hsieh, L.-W. Jian, W.-H. Chen, T.-L. Tsai and C.-F. Wang, Accurate technetium-99 determination using the combination of TEVA resin pretreatment and ICP-MS measurement and its influence on the Tc-99/Cs-137 scaling factor calculation, *J. Radioanal. Nucl. Chem.*, 2014, **299**, 1883–1889.
- 38 Triskem International, *TK201 Resin product sheet*, 2019, <https://www.triskem-international.com/catalog/products/resins-and-accessories/tk201-resin/blproduct,3922,0>, accessed 26/09/2022.
- 39 L. Skipperud, D. H. Oughton, L. S. Rosten, M. J. Wharton and P. D. Day, Determination of technetium-99 using electrothermal vaporization inductively coupled plasma-mass spectrometry (ETV-ICP-MS) and NH₄OH as chemical modifier, *J. Environ. Radioact.*, 2007, **98**(3), 251–263.
- 40 A. P. Vonderheide, M. V. Zoriy, A. V. Izmer, C. Pickhardt, J. A. Caruso, P. Ostapczuk, R. Hille and J. Sabine Becker, Determination of ⁹⁰Sr at ultratrace levels in urine by ICP-MS, *J. Anal. At. Spectrom.*, 2004, **19**, 675–680.
- 41 M. V. Zoriy, P. Ostapczuk, L. Halicz, R. Hille and J. S. Becker, Determination of ⁹⁰Sr and Pu isotopes in contaminated groundwater samples by inductively coupled plasma mass spectrometry, *Int. J. Mass Spectrom.*, 2005, **242**, 203–209.
- 42 P. Grinberg, S. Willie and R. E. Sturgeon, Determination of natural Sr and ⁹⁰Sr in environmental samples by ETV-ICP-MS, *J. Anal. At. Spectrom.*, 2007, **22**, 1409–1414.
- 43 Y. Shao, G. Yang, H. Tazoe, L. Ma, M. Yamada and D. Xu, A review of measurement methodologies and their applications to environmental ⁹⁰Sr, *J. Environ. Radioact.*, 2018, **192**, 321–333.
- 44 T. Ohno, M. Hirono, S. Kakuta and S. Sakata, Determination of strontium 90 in environmental samples by triple quadrupole ICP-MS and its application to Fukushima soil samples, *J. Anal. At. Spectrom.*, 2018, **33**, 1081–1085.
- 45 K. Nakano, Y. Shikamori, N. Sugiyama and S. Kakuta, *The ultratrace determination of iodine 129 in aqueous samples using the 7700x ICP-MS with oxygen reaction mode*, Agilent Application Note, 2012, <https://hpsst.cz/sites/default/files/oldfiles/5990-8171en-ultratrace-determination-iodine-129-aqueous-samples-using-7700x-icp-ms-oxygen-reaction.pdf>, accessed 26/09/2022.
- 46 T. Ohno, Y. Muramatsu, Y. Shikamori, C. Toyama, N. Okabe and H. Matsuzaki, Determination of ultratrace ¹²⁹I in soil samples by Triple Quadrupole ICP-MS and its application to Fukushima soil samples, *J. Anal. At. Spectrom.*, 2013, **28**, 1283–1287.
- 47 Z. Zacharuskas, P. E. Warwick, B. C. Russell, D. Reading and I. W. Croudace, Development of an Optimised Method for Measurement of Iodine-129 in Decommissioning Wastes Using ICP-MS/MS, In progress.
- 48 C.-H. Graser, N. Ial Banik, K. A. Bender, M. Lagos, C. M. Marquardt, R. Marsac, V. Montoya and H. Geckeis, Sensitive Redox Speciation of Iron, Neptunium, and Plutonium by Capillary Electrophoresis Hyphenated to Inductively Coupled Plasma Sector Field Mass Spectrometry, *Anal. Chem.*, 2015, **87**(19), 9786–9794.
- 49 C. S. Kim, C. K. Kim and K. J. Lee, Simultaneous analysis of ²³⁷Np and Pu isotopes in environmental samples by ICP-SF-MS coupled with automated sequential injection system, *J. Anal. At. Spectrom.*, 2004, **19**, 743–750.
- 50 J. Qiao, X. Hou, P. Roos and M. Miró, High-throughput sequential injection method for simultaneous determination of plutonium and neptunium in environmental solids using macroporous anion-exchange chromatography, followed by inductively coupled plasma mass spectrometric detection, *Anal. Chem.*, 2011, **83**, 374–381.
- 51 S. L. Maxwell, B. K. Culligan, A. Kelsey-Wall and P. J. Shaw, Rapid radiochemical method for determination of actinides in emergency concrete and brick samples, *Anal. Chim. Acta*, 2011, **701**, 112–118.
- 52 G. Duckworth and G. Woods, *Accurate analysis of neptunium-237 in a uranium matrix, using ICP-QQQ with MS/MS*, Agilent



- Application Note, 2012, <https://www.agilent.com/cs/library/applications/5991-6905EN.pdf>.
- 53 J. Caborn, Migration and distribution of ^{237}Np in saltmarsh sediments, PhD thesis, University of Southampton, 2015.
 - 54 A. Habibi, B. Boulet, M. Gleizes, D. Lariviere and G. Cote, Rapid determination of actinides and ^{90}Sr in river water, *Anal. Chim. Acta*, 2015, **883**, 109–116.
 - 55 F. Pointurier, N. Baglan and P. Hémet, Ultra low-level measurements of actinides by sector field ICP-MS, *Appl. Radiat. Isot.*, 2004, **60**, 561–566.
 - 56 S. Cagno, K. Hellemans, O. C. Lind, L. Skipperud, K. Janssens and B. Salbu, LA-ICP-MS for Pu source identification at Mayak PA, the Urals, Russia, *Environ. Sci.: Processes Impacts*, 2014, **16**, 306–312.
 - 57 N. Sugiyama, *Using ICP-QQQ for UO_2^+ product ion measurement to reduce uranium hydride ion interference and enable trace ^{236}U isotopic analysis*, Agilent Application Note, 2016, <https://www.agilent.com/cs/library/applications/5991-6553EN.pdf>, accessed 26/09/2022.
 - 58 B. Russell, M. Mohamud, M. Garcia Miranda, P. Ivanov, H. Thompkins, J. Scott, P. Keen and S. Goddard, Investigating the potential of tandem inductively coupled plasma mass spectrometry (ICP-MS/MS) for ^{41}Ca determination in concrete, *J. Anal. At. Spectrom.*, 2021, **36**, 845–855.
 - 59 M. Garcia Miranda, B. C. Russell and P. Ivanov, Measurement of ^{151}Sm in nuclear decommissioning samples by ICP-MS/MS, *J. Radioanal. Nucl. Chem.*, 2018, **316**, 831–838.
 - 60 DEFRA, *UK Statutory Instrument No. 0000: The Environmental Permitting (England and Wales) (Amendment) Regulations 2018*, National Radiological Protection Board, 2018.
 - 61 WHO, *Guidelines for drinking-water quality, 4th edition, incorporating the 1st addendum*, April 2017, <https://www.who.int/publications/i/item/9789241549950>, accessed 26/09/22.
 - 62 IAEA, *Safety Standards Safety Guide No. RS-G-1.7. Application of the Concepts of Exclusion, Exemption and Clearance*, https://www-pub.iaea.org/mtcd/publications/pdf/pub1202_web.pdf, accessed 03/09/2022.
 - 63 IAEA *Safety Standards Safety Guide No. RS-G-1.8. Environmental Source Monitoring for Purposes of Radiation Protection*, https://www-pub.iaea.org/MTCD/publications/PDF/Pub1216_web.pdf, accessed 03/09/2022.

